PHYSICAL REVIEW E **83**, 060701(R) (2011)

Effect of enantiomeric excess on the phase behavior of antiferroelectric liquid crystals

LiDong Pan,[1] B. K. McCoy,[1,2] Shun Wang,[1] Z. Q. Liu,[1,3] S. T. Wang,[4,5] R. Pindak,[6] and C. C. Huang[1]

[1]*School of Physics and Astronomy, University of Minnesota, Minneapolis, Minnesota 55455, USA*

[2]*Department of Mathematics and Physics, Azusa Pacific University, Azusa, California 91702, USA*

[3]*Department of Physics, Astronomy, and Engineering Science, St. Cloud State University, St. Cloud, Minnesota 56301, USA*

[4]*National Synchrotron Light Source, Brookhaven National Laboratory, Upton, New York 11973, USA*

[5]*Laboratory of Atomic and Solid State Physics, Cornell University, Ithaca, New York 14853, USA*

[6]*Photon Sciences Directorate, Brookhaven National Laboratory, Upton, New York 11973, USA*

(Received 15 March 2011; published 14 June 2011; publisher error corrected 22 June 2011)

Null transmission ellipsometry and resonant x-ray diffraction are employed to study the effect of enantiomeric excess (EE) on the phase behavior of antiferroelectric liquid crystal 10OTBBB1M7. Phase sequence, layer spacing, and pitch of the helical structures of the smectic-C^*_α and smectic-C^* phases are studied as a function of temperature and EE. Upon reducing EE, a liquid-gas-type critical point of the smectic-C^*_α to smectic-C^* transition is observed, as well as the disappearance of the smectic-C^*_{d4} and the smectic-C^*_{d3} phases. Results are analyzed in a mean-field model.

DOI: 10.1103/PhysRevE.83.060701 PACS number(s): 61.30.Hn, 77.84.Nh

The discovery of new phases and the elucidation of their structures have always been important topics in physics. However, the identification of the interactions stabilizing those structures or the forces driving the phase transitions among them can be a very challenging task. Antiferroelectric liquid-crystal (AFLC) materials and the smectic-C* (Sm C^*, in which molecules are arranged in layers and are tilted away from the layer normal) variant phases special to those materials were discovered more than two decades ago [1]. Although the structures of these phases have been established by resonant x-ray diffraction (RXRD) [2] and various optical methods [3–5], the understanding of the forces responsible for those structures and the transitions between them is still limited.

The structural model established for the Sm C^* variant phases is called the distorted clock model. Different phases are characterized by different azimuthal arrangements of tilt directions among layers. Within each layer, the tilt directions are uniform if no defects are present. The smectic-C^*_α (Sm C^*_α) and Sm C^* phase are featured with a helical structure with pitch on the order of nanometers and micrometers, respectively. The smectic-C^*_{d4} (Sm C^*_{d4}) and smectic-C^*_{d3} (Sm C^*_{d3}) phase have four-layer and three-layer unit cell structures, which are discussed in detail in Ref. [3]. The recently discovered smectic-C^*_{d6} phase has a six-layer unit cell [6].

One reason for the limited understanding of the Sm C^* variant phases is the many competing interactions involved [7], which result in a very complicated phase diagram. The phase diagram of AFLC materials is multidimensional, with temperature T, enantiomeric excess [(EE), also called optical purity], external electric field, surface anchoring strength, and concentration in a mixture system all being tunable parameters that can affect the behavior of the sample. Thus, to gain a better understanding of the physics of AFLC materials, it is beneficial to study the effects of those parameters as selectively and quantitatively as possible.

In this Rapid Communication we report our experimental results of the effect of EE on the behavior of one AFLC material. Phase sequences, transition temperatures, layer spacing, and pitch data were obtained as a function of T and EE. Although phase sequences and switching behavior have been studied as a function of EE [8–10], we are specifically reporting its effect on the temperature variation of the tilt angle and the pitch of the AFLC material. Thus our results will provide new information for understanding the behavior of AFLC materials as well as insights into the driving forces for the Sm C^* variant phases.

The material used for this study is the AFLC compound C10 (R-, optically pure) and its enatiomeric mixtures [11]. The molecular structure of C10 is shown at the top of Fig. 1. Enantiomeric mixtures were prepared by mixing R-C10 with racemic-C10. Enantiomeric excess is defined by the weight percentage of R-C10 in the mixtures. Mixtures with EE equal to 67.3%, 74%, 79.5%, 86%, and 100% (R-C10) were prepared and studied for this project.

The RXRD experiments were carried out on beam line X19A at the National Synchrotron Light Source, Brookhaven National Laboratory. Since different Sm C^* variant phases have different unit cell sizes, measurement of this quantity is essential for the study of AFLC materials. So far, RXRD remains the most powerful and most straightforward method for this task. At the resonant energy of the sulfur atom in the C10 molecule, satellite peaks appear in the q scan in addition to the Bragg peaks due to the layered structures of the smectic phases. The size of the unit cell can be determined from the relative positions of the satellite peaks and the Bragg peak. For simple helical structures such as the Sm C^*_α and the Sm C^* phases, the size of the unit cell equals the pitch of the helix. Details of the RXRD experiments have been reported elsewhere [13].

Figure 1 shows the layer spacing d as a function of T for mixtures with various values of EE. As shown in the figure, data from different samples collapse quite well onto a single curve over the temperature range studied. This indicates that the behavior of the tilt angle is not affected by the change in EE for the mixtures studied. Thus the different behaviors of Sm C^* variant phases in different samples, as shown in Fig. 2, are driven by factors other than the tilt angle evolution. This situation is very different from the results reported in Refs. [14,15], where pronounced changes in layer spacing were observed in the phase diagram.

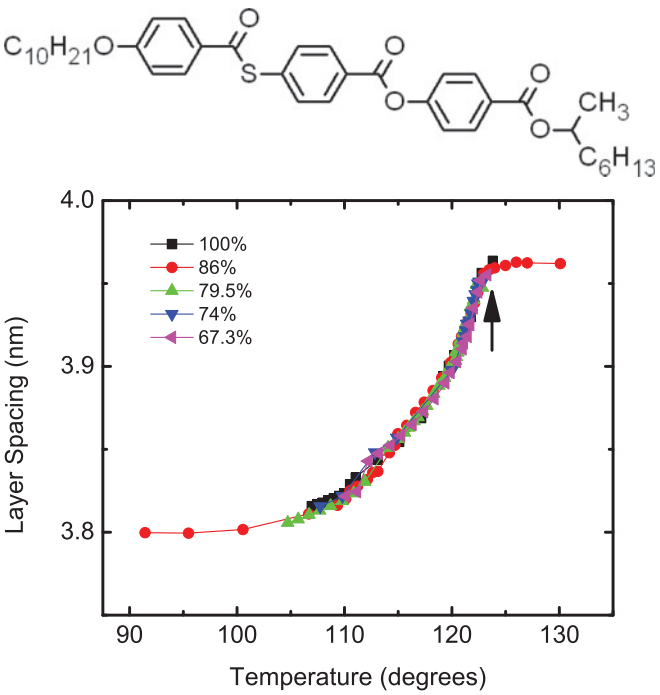

FIG. 1. (Color online) Layer spacing measured from RXRD as a function of T for different mixtures. The arrow marks the Sm A-Sm C^*_α transition temperature. Shown on top is the chemical structure of 10OTBBB1M7 (C10) [12].

Figure 2 shows the phase diagram as a function of T and EE obtained from our in-house null transmission ellipsometry (NTE) and confirmed with RXRD experiments. In the phase diagram, symbols mark the transition temperatures while lines represent phase boundaries (dashed lines were used when a phase boundary ends between data points).

Figure 2 shows the following three main features: (i) the tilt transition temperature T_{AC} is only weakly affected by the change of EE (from NTE results, about a 1 °C change in T_{AC} is observed among the different mixtures studied, while from the RXRD data, the change observed from layer spacing data in Fig. 1 seems to be smaller); (ii) as EE decreases, the Sm C^*_{d4} phase disappears first, followed by Sm C^*_{d3}, while the Sm C^* window increases; and (iii) a Sm C^*_α-Sm C^* critical point is observed in the phase diagram. While the first two behaviors have been reported elsewhere [8,9], here we observe a Sm C^*_α-Sm C^* critical point with EE and T being the two system parameters. In the following we will be focusing on the pitch evolution of the Sm C^*_α and Sm C^* phases.

Shown in Fig. 3 are the pitch evolution $P(T)$ measured from samples with different EE. As we can see from the data, mixtures with a high EE value (86% and 79.5%) exhibit a discontinuous Sm C^*_α-Sm C^* transition, where a sudden jump of pitch is observed upon cooling; mixtures with lower EE values (74% and 67.3%) exhibit continuous evolution of the pitch as we change the temperature, which indicates that those two mixtures are in the supercritical region. Since the Sm C^*_α-Sm C^* transition is a transition between short pitched structures and long pitched structures, there is no fundamental symmetry change across the transition. Thus we expect to find a liquid-gas-type critical point in the phase diagram. This critical point can be accessed by studying the pitch behavior $P(T)$ as a function of EE, with the critical mixture having an EE value between 74% and 79.5%.

Since the critical mixture is located between 74% and 79.5% EE, for mixtures with the EE value below the critical value EE_C, one cannot distinguish the Sm C^*_α phase from the Sm C^* phase. For this critical point, EE and T are the ordering fields, with EE corresponding to temperature and T corresponding to pressure in the liquid-gas transition [16]. Thus the change of pitch at the transition ΔP is a natural choice of order parameter for this transition, with $\Delta P \propto (EE_C - EE)^\beta$. For mixtures in the supercritical region, the derivative

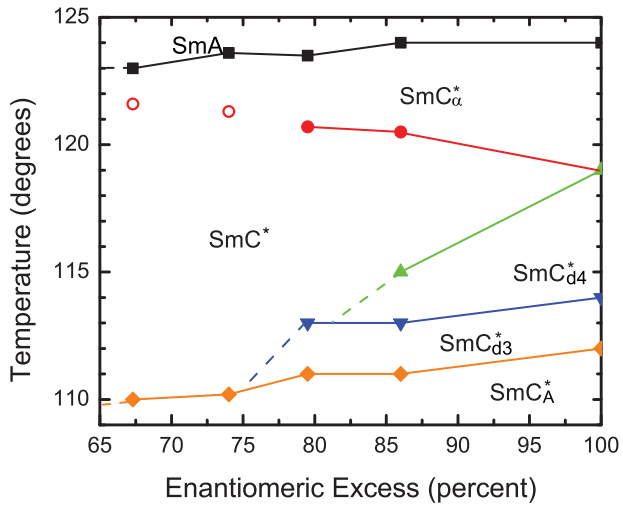

FIG. 2. (Color online) Phase diagram of C10 mixtures as a function of T and EE. Transition temperatures are marked with symbols and phase boundaries with lines. The Sm C^*_α-Sm C^* transition in the 67.3% and 74% EE mixtures are marked with open symbols to represent the supercritical nature of the transition in this region.

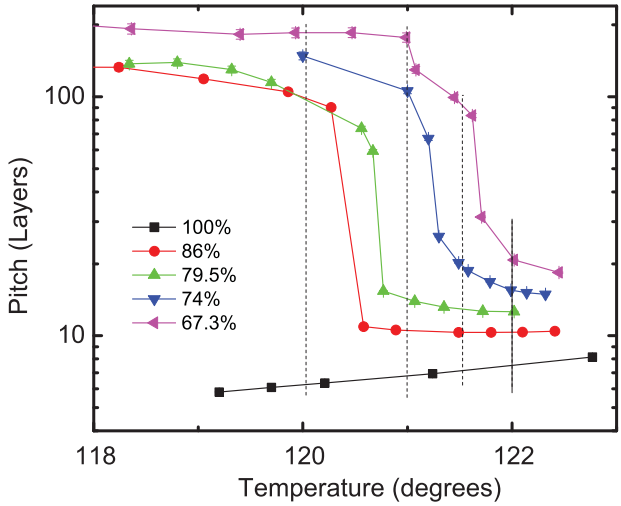

FIG. 3. (Color online) Pitch of the Sm C^*_α and the Sm C^* structures near the transition as a function of temperature and EE. Logarithmic scale is used for the vertical axis in order for the pitch behavior of the Sm C^*_α phase to be visible. Vertical dashed lines mark $T = 122$ °C, 121.5 °C, 121 °C, and 120 °C from where data in Fig. 4(a) were taken.

dP/dT would show a cusp at the crossover temperature from the short pitched SmC^*_α-like side to the long pitched SmC^*-like side. The value of dP/dT at the cusp should be a function of reduced EE as well: $dP/dT_{\rm cross} \propto ({\rm EE} - {\rm EE}_C)^{-\gamma}$. In the critical mixture with EE = EE$_C$, the evolution of the order parameter is determined by the ordering field T, with $P - P_C \propto (T - T_C)^{1/\delta}$. β, γ, and δ are all critical exponents for this transition. Since δ is expected to have the same value above and below T_C, when plotted on a log-log scale, $|P - P_C|$ as a function of $|T - T_C|$ is expected to be parallel for $T > T_C$ and $T < T_C$ [11]. This rule of phase transition should be followed when choosing the order parameter and determining the position of the critical point [17].

To the best of our knowledge, there are at least three different routes that allow one to explore the SmC^*_α-SmC^* critical point. One is the method we report in this paper, by reducing the EE of C10. The second one is by studying mixtures of compounds showing first-order and supercritical SmC^*_α-SmC^* transitions [18]. Here we argue the first method is superior because it minimizes the complications introduced by the different SmA-SmC^*_α transition temperatures in the mixtures with other compounds. Thus, for the second method, it is not possible to perform scaling analysis of the data. Although for our experiments we do not have sufficient data density or mixtures with different EE values to perform a scaling analysis, it is in principle doable. The third possible method to study the SmC^*_α-SmC^* critical behavior would be to perform a pitch measurement on a sample with a weakly first-order SmC^*_α-SmC^* transition. By studying the pitch behavior as a function of temperature and external transverse field (which has been shown to unwind the helix of the SmC^*_α and SmC^* structures), a complete picture of the SmC^*_α-SmC^* critical point could be obtained.

To gain further understanding of the experimental results, we employ a simple model for the helical structures. The relevant free energy is

$$F = J_1 \sum_{i=1}^{n} \boldsymbol{\xi}_i \cdot \boldsymbol{\xi}_{i+1} + J_2 \sum_{i=1}^{n} \boldsymbol{\xi}_i \cdot \boldsymbol{\xi}_{i+2}, \qquad (1)$$

where J_1 is the nearest-neighbor (NN) interlayer interaction, J_1 can be either ferroelectric or antiferroelectric, J_2 is the antiferroelectric next-nearest-neighbor (NNN) interlayer interaction, and $\boldsymbol{\xi}_i$ is a unit vector describing the tilt direction of the ith layer. The frustration between the NN and the NNN interlayer interactions will produce a helical structure, with an angle ϕ between neighboring layers given by

$$\cos(\phi) = -J_1/4J_2, \qquad (2)$$

with $-1 \leqslant J_1/4J_2 \leqslant 1$.

Several previous studies have shown that the J_1-J_2 model is too simple to describe the SmC^*_α-SmC^* transition [19,20]; and for samples showing a first-order SmC^*_α-SmC^* transition (79.5% and 86%), it requires a discontinuity in the temperature evolution of the J_2/J_1 value, which is quite unphysical. However, a satisfactory theory for the SmC^*_α-SmC^* transition is presently unavailable. Thus the J_1-J_2 model can still give useful information about the behaviors observed with different EE values.

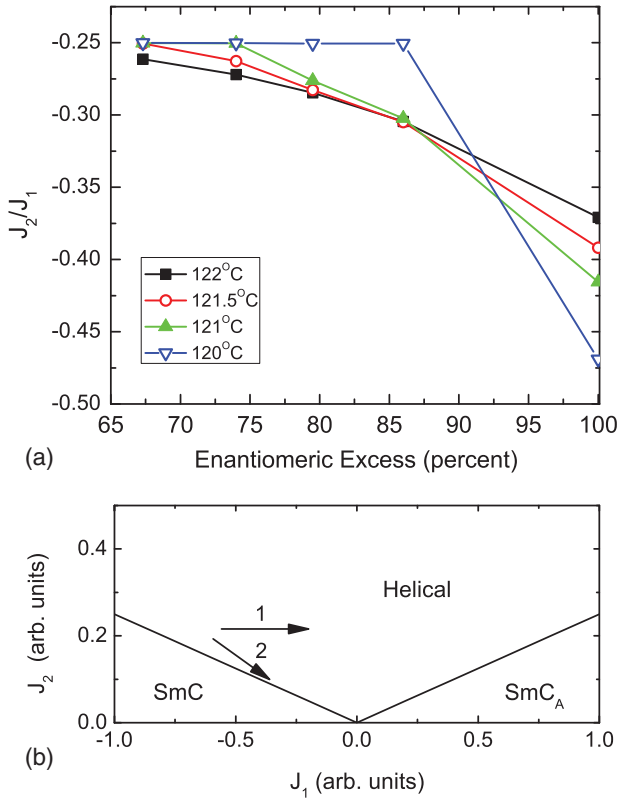

FIG. 4. (Color online) (a) J_2/J_1 as a function of EE calculated from Eq. (2) and pitch data obtained at $T = 120\,^\circ$C, $121\,^\circ$C, $121.5\,^\circ$C, and $122\,^\circ$C. (b) Phase diagram of the J_1-J_2 model. Arrows 1 and 2 illustrate the behavior upon cooling of the optically pure sample and samples with a low EE value, respectively. The arrows point to lower temperature.

From Eq. (2) and Fig. 3 we obtain Fig. 4(a), which shows the value of J_2/J_1 calculated from $P(T)$ data obtained from mixtures with different EE values at $T = 120\,^\circ$C, $121\,^\circ$C, $121.5\,^\circ$C, and $122\,^\circ$C. We can see from the figure that, not only does the value of $|J_2/J_1|$ decrease with decreasing EE value, but the temperature derivative of $|J_2/J_1|$ also changes sign upon reducing the EE. In the optically pure sample, no SmC^* phase was observed and the pitch in SmC^*_α phase shows a monotonic decrease upon cooling. This gives a $|J_2/J_1|$ that increases monotonically with decreasing temperature. However, from samples with a low EE value (67.3% and 74%), there is a monotonic decrease of the $|J_2/J_1|$ value upon cooling. These different behaviors are illustrated in Fig. 4(b) with two arrows.

Figure 4(b) shows the phase diagram of the J_1-J_2 model. In this model there are three phases: SmC, SmC_A, and the helical phase (corresponding to both SmC^*_α and SmC^*). (Since no chiral interaction is considered in this model, the resulting structures are not chiral.) Arrows 1 and 2 represent the behavior of the optically pure sample and the 67.3% and 74% EE samples, respectively, upon cooling. As shown in this figure, a change of EE in AFLC materials not only changes the position of the sample in the phase diagram, but can also completely change the direction of the sample's temperature evolution.

In Fig. 4(a) the value of $|J_2/J_1|$ shows a monotonic decrease with decreasing EE. Although, due to the limitation of the

J_1-J_2 model, there is a lower bound of 0.25 for the value of $|J_2/J_1|$ calculated from the data, this observation still bears important information. First, with decreased EE, the pitch of the helical structure increases. This indicates a reduced twisting power of the liquid-crystal sample and is consistent with the understanding that the twisting power of liquid-crystal materials is related to the net sample chirality or optical purity. Second, a reduction of the $|J_2/J_1|$ value suggests a reduced level of frustration in mixtures with lower EE values. Although presently there is no satisfying theory for the formation of the Sm C^* variant phases in AFLC materials, it is generally agreed that frustration between different interactions is responsible for the intermediate phases and structures observed. A decreased level of frustration would thus results in lowered stability of those phases, as observed in Fig. 2. Although the model used is still rough, our results give a quantitative account of the phase behavior of AFLC as a function of EE.

To summarize, we studied the effect of enantiomeric excess on the behavior of Sm C^* variant phases in the compound C10. We found that with decreasing EE value, (i) the Sm C^* variant phases give way to Sm C^*, (ii) the pitch of the helical structure increases, and (iii) a liquid-gas-type critical point of the Sm C^*_α-Sm C^* transition was observed. By analyzing the data with a simple J_1-J_2 model, we found that those observations indicate a reduced twisting power and decreased level of frustration when EE is lowered.

This research was supported in part by the National Science Foundation, Solid State Chemistry Program, under Grant No. DMR-0605760. Use of the National Synchrotron Light Source, Brookhaven National Laboratory, was supported by the US Department of Energy, Office of Science, Office of Basic Energy Sciences, under Contract No. DE-AC02-98CH10886. L.D.P. acknowledges financial support from University of Minnesota Graduate School in the final stage of this project. The authors would like to thank Dr. P. Barois for lending us the oven for the x-ray experiments and Dr. H. T. Nguyen for supplying the high-quality C10 compounds.

[1] T. Niori *et al.*, J. Mater. Chem. **6**, 1231 (1996).
[2] P. Mach *et al.*, Phys. Rev. Lett. **81**, 1015 (1998).
[3] P. M. Johnson *et al.*, Phys. Rev. Lett. **84**, 4870 (2000).
[4] D. Konovalov, H. T. Nguyen, M. Copic, and S. Sprunt, Phys. Rev. E **64**, 010704(R) (2001).
[5] M. Škarabot *et al.*, Phys. Rev. E **58**, 575 (1998).
[6] S. Wang *et al.*, Phys. Rev. Lett. **104**, 027801 (2010).
[7] R. Bruinsma and J. Prost, J. Phys. II **4**, 01209 (1994).
[8] A. Cady *et al.*, Phys. Rev. E **66**, 061704 (2002).
[9] E. Gorecka, D. Pociecha, M. Cepic, B. Zeks, and R. Dabrowski, Phys. Rev. E **65**, 061703 (2002).
[10] M. R. Dodge and C. Rosenblatt, Phys. Rev. E **62**, 6891 (2000).
[11] The following is the phase sequence reported for R-C10: isotropic (153 °C) Sm A (124 °C) Sm C^*_α (120 °C) Sm C^* (119 °C) Sm C^*_{d4} (114 °C) Sm C^*_{d3} (112 °C) Sm C^*_A (110 °C) crystal. However, no Sm C^* phase was observed in R-C10 from RXRD or NTE.
[12] Data for the mixture with 86% EE has been shifted down by 0.02 nm; the difference from other mixtures is probably due to the difference in the calibration of the setup.
[13] P. Mach *et al.*, Phys. Rev. E **60**, 6793 (1999).
[14] S. Jaradat *et al.*, J. Mater. Chem. **16**, 3753 (2006).
[15] J. Kirchhoff and L. S. Hirst, Phys. Rev. E **76**, 051704 (2007).
[16] M. E. Fisher, in Critical Phenomena, edited by F. J. W. Hahne, Lecture Notes in Physics Vol. 186 (Springer-Verlag, Berlin, 1983), Chap. 1.
[17] For the choice of order parameter and determination of the critical point, the authors of Ref. [18] argued that on the critical isotherm, the behavior of the order parameter should be symmetric about critical point, i.e., the ratio of the critical amplitude should be one. This puts an additional, unnecessary constraint on the data analysis. Under this constraint, the square root of the pitch was chosen as the quantity related to the order parameter in Ref. [18].
[18] Z. Q. Liu *et al.*, Phys. Rev. E **74**, 030702 (2006).
[19] A. Cady *et al.*, Phys. Rev. E **65**, 030701 (2002).
[20] V. P. Panov, D. A. Olson, X. F. Han, H. T. Nguyen, and C. C. Huang, Phys. Rev. E **74**, 011701 (2006).